A Comparison of the Bioconversion Rates and the Caco-2 Cell Permeation Characteristics of Coumarin-Based Cyclic Prodrugs and Methylester-Based Linear Prodrugs of RGD Peptidomimetics

Gian P. Camenisch,[1] Wei Wang,[2] Binghe Wang,[2,3] and Ronald T. Borchardt[1,3]

Received February 27, 1998; accepted May 1, 1998

Purpose. To compare the bioconversion rates in various biological media and the Caco-2 cell permeation characteristics of coumarin-based cyclic prodrugs (3a, 3b) and methylester-based linear prodrugs (1b, 2b) of two RGD peptidomimetics (1a, 2a).

Methods. Bioconversion rates of the prodrugs to the RGD peptidomimetics were determined in Hank balanced salt solution (HBSS), pH 7.4, at 37°C and in various biological media (human blood plasma, rat liver homogenate, Caco-2 cell homogenate) known to have esterase activity. Transport rates of the prodrugs and the RGD peptidomimetics were determined using Caco-2 cell monolayers, an *in vitro* cell culture model of the intestinal mucosa.

Results. In HBSS, pH 7.4, the coumarin-based cyclic prodrugs 3a and 3b degraded slowly and quantitatively to the RGD peptidomimetics 1a and 2a, respectively (3a, $t_{1/2} = 630 \pm 14$ min; 3b, $t_{1/2} = 301 \pm 12$ min). The methylester-based linear prodrugs 1b and 2b were more stable to chemical hydrolysis (1b and 2b, $t_{1/2} > 2000$ min). Both the coumarin-based cyclic prodrugs and the methylester-based linear prodrugs degraded more rapidly in biological media containing esterase activity (e.g., 90% human blood plasma: 1b, $t_{1/2} < 5$ min; 2b, $t_{1/2} < 5$ min; 3a, $t_{1/2} < 91 \pm 1$ min; 3b, $t_{1/2} < 57 \pm 2$ min). When the apical (AP)-to-basolateral (BL) permeation characteristics were determined using Caco-2 cell monolayers, it was found that the methylester prodrugs 1b and 2b underwent esterase bioconversion (>80%) to the RGD peptidomimetics 1a and 2a, respectively. In contrast, the cyclic prodrugs 3a and 3b permeated the cell monolayers intact. Considering the appearance of both the prodrug and the RGD peptidomimetic on the BL side, the methylester prodrugs 1b and 2b were approximately 12-fold more able to permeate than were the RGD peptidomimetics 1a and 2a. When a similar analysis of the transport data for the coumarin prodrugs 3a and 3b was performed, they were shown to be approximately 6-fold and 5-fold more able to permeate than were the RGD peptidomimetics 1a and 2a, respectively.

Conclusions. The coumarin-based cyclic prodrugs 3a and 3b were chemically less stable, but metabolically more stable, than the methylester-based linear prodrugs. The esterase stability of the cyclic prodrugs 3a and 3b means that they are transported intact across the Caco-2 cell monolayer in contrast to the methylester prodrugs 1b and 2b, which undergo facile bioconversion during their transport to the RGD peptidomimetics. However, both prodrug systems successfully delivered more (5-12-fold) of the RGD peptidomimetic and/or the precursor (prodrug) than did the RGD peptidomimetics themselves.

KEY WORDS: esterase-sensitive prodrugs; peptidomimetic; chemical and enzymatic stability; Caco-2 cells; membrane permeability; drug delivery.

INTRODUCTION

RGD (Arg-Gly-Asp) peptidomimetics, which are fibrinogen antagonists, are promising platelet aggregation inhibitors (1). These peptidomimetics have unique pharmacological properties that warrant their eventual development as therapeutic agents in treating and preventing related cardiovascular diseases or complications such as stroke, myocardial infarction, or peripheral diseases (2–4). However, one major problem in developing these RGD peptidomimetics into therapeutically useful agents is their low oral bioavailability (3,5,6).

The oral bioavailability of drug compounds is influenced by many factors, including dissolution, absorption, pre-systemic and systemic metabolism, and elimination. The low oral bioavailability of RGD peptidomimetics is thought to be influenced mainly by unfavorable physicochemical properties (i.e., charge and high polarities) that prevent these compounds from permeating biological barriers such as the intestinal mucosa (3,5,6). The major contributor to the charge and high polarities of RGD peptidomimetics is the presence of both *C*-terminal carboxyl and *N*-terminal amino groups in these compounds, which give the molecules their affinity and specificity for the pharmacological receptor (6). Little is known about the liver and kidney clearance of RGD peptidomimetics in humans (7). However, pharmacokinetic data generated in animals (dog, monkey, rat, etc.) indicate a high rate of elimination of these compounds by the kidney and the liver (8–12).

Various prodrug strategies have been employed to transiently alter the unfavorable physicochemical properties of RGD peptidomimetics in order to overcome their absorption problems. Prodrug approaches to enhance the oral permeability of RGD peptidomimetics have generally used traditional methodologies, i.e. transiently masking the C-terminal carboxyl and/or the N-terminal amino functional groups of the compounds. For example, Hutchinson et al. (13) prepared the ethyl ester prodrugs of some 3,4-dihydro-1(1H)-isoquinolinone-based RGD peptidomimetics and showed that these prodrugs have oral bioavailabilities in dogs of at least 17%. Weller et al. (14) prepared the amidoxime ester prodrug of the RGD peptidomimetic Ro48-3657, which was absorbed approximately 20 times better after oral administration to mice than was the parent drug.

A promising, new approach to the development of peptide prodrugs is the bioreversible cyclization of the peptide backbone (15). Our laboratories have developed various promoieties to achieve this bioreversible cyclization, including an acyloxyalkoxy promoiety (16,17), a phenylpropionic acid promoiety (16,18) and a coumarin-based promoiety (19,20). The resulting cyclic prodrugs have been shown to be susceptible to esterase metabolism (slow step), leading to a cascade of chemical reactions and resulting in generation of the parent peptide (17,20).

The purpose of this study was to evaluate the impact of the coumarin-based promoiety on the cell membrane permeability of RGD peptidomimetics. The impact of the coumarin-based

[1] Department of Pharmaceutical Chemistry, The University of Kansas, Lawrence, Kansas 66047.

[2] Department of Chemistry, North Carolina State University, Raleigh, North Carolina 27695-8204.

[3] To whom correspondence should be addressed. (e-mail: borchardt@smissman.hbc.ukans.edu)

0724-8741/98/0800-1174$15.00/0

cyclic prodrug strategy was compared to the more traditional approach of preparing a methylester-based linear prodrug.

MATERIALS

Chemicals

The two RGD-mimetics and the corresponding methylester-based linear prodrugs were prepared according to literature procedures (1). The coumarin-based cyclic prodrugs were prepared as described elsewhere (21).

Diethyl *p*-nitrophenyl phosphate (paraoxon, approx. 90%), *p*-nitrophenyl butyrate (approx. 98%), dimethyl sulfoxide (>99.5%), Dulbecco's phosphate buffered saline, and Hanks' balanced salts (modified) were purchased from Sigma Chemical Co. (St. Louis, MO). L-Glutamine (200 mM, 100×), penicillin (10,000 U/ml), streptomycin (10,000 μg/ml), and non-essential amino acids (10 mM, 100×) in 0.85% saline were obtained from Gibco BRL, Life Technologies (Grand Island, NY). Dulbecco's modified Eagle medium and trypsin/EDTA solution (0.25% and 0.02%, respectively, in Ca^{2+}- and Mg^{2+}-free HBSS) were purchased from JRH Biosciences (Lenexa, KS). Rat tail collagen (type I) was obtained from Collaborative Biomedical Products (Bedford, MA), and fetal bovine serum from Atlanta Biologicals (Norcross, GA). All other chemicals and solvents were of high purity or analytical grade and used as received.

METHODS

Enzymatic and Chemical Stability Experiments

General Protocol for Chemical Stability Studies

The chemical stabilities of the prodrugs were determined in HBSS, pH 7.4. Solutions of the prodrugs (~1 mM) were incubated in sealed vials at 37.0 ± 0.5°C in a temperature-controlled shaking water bath (60 rpm). Periodically, 20 μl aliquots were removed and immediately analyzed for the presence of remaining prodrug and degradation products (coumarin and/or RGD peptidomimetics, respectively) by HPLC. Apparent half-lives ($t_{1/2}$) for the disappearance of the prodrugs were calculated by linear regression ($r^2 \geq 0.96$) from pseudo-first-order plots of prodrug concentration vs. time measured up to 1440 min.

General Protocol for Enzymatic Stability Studies

The stabilities of the prodrugs in 90% human plasma, Caco-2 transport buffers, and various tissue homogenates were determined at 37°C in the presence and absence of paraoxon, a potent esterase inhibitor. The determination of total esterase activity in these biological media using *p*-nitrophenyl butyrate (PNPB) has been extensively described elsewhere (17). The prodrugs were incubated at ~100 μM with the biological matrix, and samples were maintained for 6 hr in a temperature-controlled (37.0 ± 0.5°C) shaking water bath (60 rpm). To test the effect of an esterase inhibitor on the rate of degradation of the prodrugs, the final medium was preincubated with paraoxon (final concentration 1 mM) for 15 min at 37°C before adding the prodrug. At various times, aliquots (20 μl) were removed and the esterase activity immediately quenched by adding 150 μl of a freshly prepared 6 N guanidinium hydrochloride solution in acidified HBSS [HBSS containing 0.01% (v/v) phosphoric acid]. Aliquots (150 μl) of the acidic mixture (pH ~3) were then transferred to an Ultrafree®-MC 5000 NMWL filter unit (Millipore, Bedford, MA) and centrifuged at 7500 rpm (5000 ×g) for 60 min (4°C). Aliquots (50 μl) of the filtrates were diluted with mobile phase and analyzed for the presence of remaining prodrug and degradation products (coumarin and/or RGD peptidomimetics, respectively) on the HPLC column. $T_{1/2}$ values for the disappearance of the prodrug were calculated from the rate constants obtained by linear regression ($r^2 \geq 0.91$) from pseudo-first-order plots of prodrug concentration vs. time.

Preparation of Biological Media

Rat Liver Homogenate. Rat livers were obtained from male Sprague-Dawley rats (Animal Care Unit, The University of Kansas, Lawrence, KS) weighing 250–350 g. The tissue was prepared as described previously (17). Homogenates were prepared in HBSS (1 ml per g tissue) as described elsewhere (17).

Caco-2 Cell Homogenate. Confluent Caco-2 cell monolayers (21–28 days) were washed 3× with ice-cold HBSS and carefully scraped from the filter support with a rubber spatula. Cells of 6 monolayers were collected in 2 ml of ice-cold HBSS and the homogenates were prepared as described previously (17).

90% Human Plasma. Human blood, stabilized with CPDA-1 solution USP, was obtained from the Topeka Blood Bank (Topeka, KS). Plasma was separated from erythrocytes at 4°C by centrifugation for 10 min at 4700 rpm (2000 × g). For stability studies, human plasma was diluted to 90% (v/v) with HBSS, pH 7.4, in order to maintain the pH of the solution during the experiment.

Caco-2 Transport Buffer. Confluent Caco-2 cell monolayers (21–28 days) were incubated with HBSS, pH 7.4, at 37°C. After exactly 3 hours, aliquots of AP and BL transport buffers were collected separately.

Caco-2 Transport and Uptake Experiments

Cell Culturing Methodology

Caco-2 cells (passage 18) were obtained from American Type Culture Collection (Rockville, MD) and cultured as described previously (17,22). Cells used in this study were between passages 35 and 50.

Transport Experiments

Caco-2 cell monolayers grown on collagen-coated polycarbonate filters (Transwells®) for 21 to 28 days were used for transport experiments. The integrity of each batch of cells was tested by measuring the flux of [^{14}C]-mannitol in representative cell monolayers (n = 3). AP-to-BL flux for this paracellular marker never exceeded values of 0.4%/hr ($P_e \leq 1.27 \cdot 10^{-7}$ cm/s). The transport of the compounds across the Caco-2 cell monolayers was determined as described earlier (17). Briefly, the compound solution (90–100 μM in HBSS) was applied to the donor compartment (AP, 1.5 ml or BL, 2.6 ml) of the cell

monolayer and HBSS was added to the receiver compartment. Samples (120 μl receiver side and 20 μl donor side) were removed from both sides at various times up to 180 min. The volume removed from the receiver side was always replaced with fresh, prewarmed HBSS. Samples were stabilized with an aliquot of acetonitrile and diluted phosphoric acid [final concentration 10% (v/v) and 0.01% (v/v), respectively] and kept frozen (−80°C) until HPLC analysis. Transport experiments from the AP-to-BL side as well as from the BL-to-AP side were performed in triplicates at 37°C in an incubator (average ± SD).

Uptake Experiments

To check mass balance, the uptake of the compounds in Caco-2 cells was determined. Immediately after performing transport studies, the transport medium was removed and the cells were washed 3 times with ice-cold HBSS, pH 7.4, to stop further uptake and to remove unbound compound. Subsequently, the cells were scraped from the polycarbonate filters into a 0.01 N HCl:ethanol solution [50:50% (v/v)]. After sonication, aliquots of the acidic mixture (pH ~3) were centrifuged at 13,000 rpm (8600 × g) for 5 min (4°C). Samples were then analyzed by HPLC (see HPLC Analysis section below).

HPLC Analysis

Chromatographic analyses were carried out on a Shimadzu LC-6A gradient system (Shimadzu, Inc., Tokyo, Japan) consisting of LC-6A pumps, a SCL-6A and a SCL-10A controller, a SPD-6A UV detector and a SIL-10A autoinjector. Samples from a refrigerated sample tray (4°C) were injected on a Dynamax C_{18} reversed-phase column (5 μm, 300 Å, 25 cm × 4.6 mm I.D., Rainin Instruments, Woburn, MA) equipped with a guard column. The RGD peptidomimetics and the corresponding methylester-based prodrugs were detected at a wavelength of 276 nm, whereas the coumarin-based prodrugs were detected at a wavelength of 254 nm. Gradient elution (20 min) of the compounds was performed at a flow rate of 1 ml/min from 10.0–90.0% (v/v) acetonitrile in water using trifluoroacetic acid [0.1%, (v/v)] as the ion-pairing agent.

Data Analysis

Permeability coefficients (P_e) of the compounds were calculated according to Eq. 1:

$$P_e = \frac{\Delta Q/\Delta t}{A \cdot c(0)} \quad (1)$$

where $\Delta Q/\Delta t$ = linear appearance rate of mass in the receiver solution, A = cross-sectional area (i.e., 4.71 cm^2), and c(0) = initial compound concentration in the donor compartment at t = 0.

RESULTS

Chemical and Enzymatic Stability

The chemical and enzymatic degradation kinetics of the linear prodrugs 1b and 2b and the cyclic prodrugs 3a and 3b, respectively, were followed for at least two half-lives. For the methylester-based prodrugs 1b and 2b, the only degradation products were the RGD peptidomimetics 1a and 2a, respectively. For the coumarin-based prodrugs 3a and 3b, the RGD peptidomimetics 1a and 2a, respectively, as well as coumarin appeared as degradation products. By analyzing for the presence of remaining prodrug and degradation products (coumarin and/or RGD peptidomimetics, respectively) mass balance (>95%) was achieved in all experiments. $T_{1/2}$ values of all the prodrugs are presented in Tables I and II. The results show that the rates of disappearance of the cyclic prodrugs 3a and 3b, when incubated in human plasma or rat liver homogenate, are significantly faster than the rates observed in HBSS, Caco-2 transport buffer (AP or BL) and Caco-2 cell homogenate. Although some esterase activity was determined in Caco-2 cell homogenate (Tables I and II), the $t_{1/2}$ values of cyclic prodrugs 3a and 3b were similar to the $t_{1/2}$ values determined in HBSS. In contrast, the linear methylester-based prodrugs 1b and 2b degraded faster in all the biological media studied than in HBSS. In human plasma, Caco-2 cell homogenate and rat liver homogenate, linear prodrugs 1b and 2b disappeared within <15 min.

Incorporation of paraoxon, a potent esterase inhibitor, in the various biological media used in these experiments generally resulted in a substantial decrease in the specific esterase activity (Tables I and II). Based on the spectrophotometric assay, using *p*-nitrophenyl butyrate as substrate, residual esterase activity after 15 min preincubation with paraoxon at 37°C was <3%, except in 90% human blood plasma and in Caco-2 cell homogenate, where the activity was only reduced to 43% and 13%, respectively. However, in the presence of paraoxon, the rates of disappearance of both the coumarin-based and the methylester-based prodrugs in rat liver homogenate and in 90% human blood plasma were significantly different from the respective degradation rates observed for chemical degradation in HBSS.

Transport Across Caco-2 Cell Monolayers

Permeation through Caco-2 cell monolayers, an *in vitro* model of the intestinal mucosa, was assessed for the two RGD peptidomimetics (1a and 2a) and the corresponding coumarin-based (3a and 3b) and methylester-based (1b and 2b) prodrugs. After determining uptake into the cells at the completion of the transport experiments, mass balance (>91%) was achieved in all experiments (data not shown). Permeability coefficients for the compounds considered in this study are presented in Table III.

Both RGD peptidomimetics 1a and 2a exhibited poor permeation through the Caco-2 cell monolayer. The mass balance experiments revealed that after 180 min about 95% of the RGD peptidomimetics remained in the donor compartment. About 3.5% of the RGD peptidomimetics could be found within the cells. The P_e values for the RGD peptidomimetics in the BL-to-AP direction were not statistically different from those observed for the flux in the AP-to-BL direction.

Considering only the appearance of prodrug in the receiver compartment, the coumarin-based cyclic prodrug 3a was about 5.3-fold more able to permeate the cell monolayer than was the corresponding RGD peptidomimetic 1a. For cyclic prodrug 3b, the difference in permeation from the corresponding RGD peptidomimetic 2a was about 3.9-fold. The permeabilities determined in the BL-to-AP direction for the coumarin-based prodrugs 3a and 3b were not statistically different from those observed for the flux of the compounds in the AP-to-BL direc-

Table I. Apparent Half-Lives ($t_{1/2}$) of the Prodrugs 3a and 1b in HBSS (pH 7.4) and Different Biological Media in the Presence and Absence of Paraoxon (1 mM) at 37°C

Incubation Mixture	Specific Activity[a] [U/mg]	Enzyme Concentration [U/ml]		$t_{1/2}$ for 3a[b] [min]		$t_{1/2}$ for 1b[b] [min]	
		− paraoxon	+ paraoxon	− paraoxon	+ paraoxon	− paraoxon	+ paraoxon
HBSS, pH 7.4	0	0	0	630 ± 14	626 ± 12	>2000	>2000
AP HBSS, pH 7.4	0.44	0.06	0	625 ± 9	628 ± 6	1479 ± 15	>2000
BL HBSS, pH 7.4	0.46	0.04	0	627 ± 11	628 ± 5	1633 ± 18	>2000
Caco-2 cell homogenate	0.37	0.30	0.04	615 ± 15	635 ± 14	12 ± 2	>2000
90% human blood plasma	0.08	0.51	0.22	91 ± 1	146 ± 5	<5	272 ± 3
Rat liver homogenate	1.09	5.63	0.13	42 ± 2	495 ± 12	<<5	834 ± 9

[a] Determined at 25°C in HBSS, pH 7.4 using *p*-nitrophenyl butyrate as substrate.
[b] Calculated from apparent first-order rate constants.

Table II. Apparent Half-Lives ($t_{1/2}$) of the Prodrugs 3b and 2b in HBSS (pH 7.4) and Different Biological Media in the Presence and Absence of Paraoxon (1 mM) at 37°C

Incubation Mixture	Specific Activity[a] [U/mg]	Enzyme Concentration [U/ml]		$t_{1/2}$ for 3b[b] [min]		$t_{1/2}$ for 2b[b] [min]	
		− paraoxon	+ paraoxon	− paraoxon	+ paraoxon	− paraoxon	+ paraoxon
HBSS, pH 7.4	0	0	0	301 ± 12	296 ± 4	>2000	>2000
AP HBSS, pH 7.4	0.44	0.06	0	291 ± 3	298 ± 4	1155 ± 12	>2000
BL HBSS, pH 7.4	0.46	0.04	0	292 ± 7	296 ± 6	1387 ± 7	>2000
Caco-2 cell homogenate	0.37	0.30	0.04	277 ± 8	315 ± 9	5	1562 ± 18
90% human blood plasma	0.08	0.51	0.22	57 ± 2	97 ± 2	5	182 ± 4
Rat liver homogenate	1.09	5.63	0.13	38 ± 3	203 ± 8	<<5	577 ± 6

[a] Determined at 25°C in HBSS, pH 7.4 using *p*-nitrophenyl butyrate as substrate.
[b] Calculated from apparent first-order rate constants.

Table III. Transport Characteristics for RGD Peptidomimetics 1a and 2a, the Methylester-based Prodrugs 1b and 2b, and the Coumarin-based Prodrugs 3a and 3b Across Caco-2 Cell Monolayers

Compound	Permeability Coefficient [cm/s]	
	AP-to-BL	BL-to-AP
RGD Peptidomimetic 1a	3.94E-07 ± 5.03E-09	3.99E-07 ± 4.11E-08
Cyclic Prodrug 3a: - Appearance of Prodrug[a]	2.06E-06 ± 2.62E-07	2.12E-06 ± 3.75E-07
- Appearance of RGD Peptidomimetic[b]	3.61E-07 ± 2.49E-08	3.52E-07 ± 2.37E-08
- Appearance of Prodrug and RGD Peptidomimetic[c]	2.42E-06 ± 2.87E-07	2.47E-06 ± 3.99E-07
Linear Prodrug 1b: - Appearance of Prodrug[a]	2.05E-08 ± 8.03E-09	3.20E-07 ± 2.60E-08
- Appearance of RGD Peptidomimetic[b]	4.59E-06 ± 3.43E-07	1.89E-05 ± 9.39E-07
- Appearance of Prodrug and RGD Peptidomimetic[c]	4.61E-06 ± 3.51E-07	1.92E-05 ± 9.65E-07
RGD Peptidomimetic 2a	3.88E-07 ± 1.00E-08	3.86E-07 ± 2.15E-08
Cyclic Prodrug 3b: - Appearance of Prodrug[a]	1.48E-06 ± 1.85E-07	1.52E-06 ± 3.84E-07
- Appearance of RGD Peptidomimetic[b]	4.19E-07 ± 2.89E-08	4.22E-07 ± 2.74E-08
- Appearance of Prodrug and RGD Peptidomimetic[c]	1.90E-06 ± 2.14E-07	1.94E-06 ± 4.11E-07
Linear Prodrug 2b: - Appearance of Prodrug[a]	3.37E-07 ± 8.80E-09	1.74E-06 ± 6.39E-08
- Appearance of RGD Peptidomimetic[b]	4.22E-06 ± 1.39E-07	1.74E-05 ± 8.44E-07
- Appearance of Prodrug and RGD Peptidomimetic[c]	4.56E-06 ± 1.48E-07	1.91E-05 ± 9.08E-07

[a] Permeability coefficients are calculated according to Eq. 1, taking into account the linear appearance of the prodrug only.
[b] Permeability coefficients are calculated according to Eq. 1, taking into account the linear appearance of the RGD peptidomimetic only.
[c] Permeability coefficients are calculated according to Eq. 1, taking into account the linear appearance of both the prodrug and the RGD peptidomimetic.

tion. In addition to the cyclic prodrugs 3a and 3b, a significant amount of RGD peptidomimetics 1a and 2a could be detected in the receiver compartment (Fig. 2B). Taking into account the amount of both the prodrug and RGD peptidomimetic, cyclic prodrug 3a was about 6.2-fold more able to "deliver" the prodrug and the RGD peptidomimetic across the Caco-2 cells than was the RGD peptidomimetic itself. For cyclic prodrug 3b, the difference in apparent permeation from the corresponding RGD peptidomimetic 2a was about 5.0-fold. In contrast to the parent RGD peptidomimetics 1a and 2a, the coumarin-based prodrugs 3a and 3b disappeared quite rapidly from the donor compartment. The mass balance studies showed that after 180 min only about 47% of the prodrugs remained in the donor compartment (Fig. 2A). Approximately 33% of the prodrugs could be found within the cells.

Considering only the appearance of prodrugs in the receiver compartment, the methylester-based linear prodrugs 1b and 2b exhibited very low permeation. The amount of prodrugs 1b and 2b transported to the receiver compartment within 180 min was generally less than that for the parent RGD peptidomimetics 1a and 2a (< 1%). However, since the methylester prodrugs 1b and 2b underwent rapid hydrolysis in Caco-2 cells, large amounts of the RGD peptidomimetics 1a and 2a were detected in the receiver compartment when the prodrugs were administered to the donor compartment (Fig. 3A and 3B). Considering the amount of prodrug and RGD peptidomimetic, both methylester prodrugs 1b and 2b were about 11.7-fold more able to permeate the Caco-2 cell monolayer in the AP-to-BL direction than were the corresponding RGD peptidomimetics 1a and 2a. For the BL-to-AP transport, the apparent differences in permeation were about 49-fold. As shown in Figure 3A, the linear prodrugs disappeared rapidly from the donor compartment. The mass balance results showed that after 180 min only about 2% and 19% of the prodrugs remained in the donor compartment for the AP-to-BL and BL-to-AP transport, respectively. After the same time period, about 67% (for AP-to-BL transport) and 55% (for BL-to-AP transport) parent RGD peptidomimetics could be detected in the donor compartment. Only negligible amounts of methylester-based prodrugs (<1%) could be found within the cells for both transport directions, whereas about 16% of the RGD peptidomimetics were present.

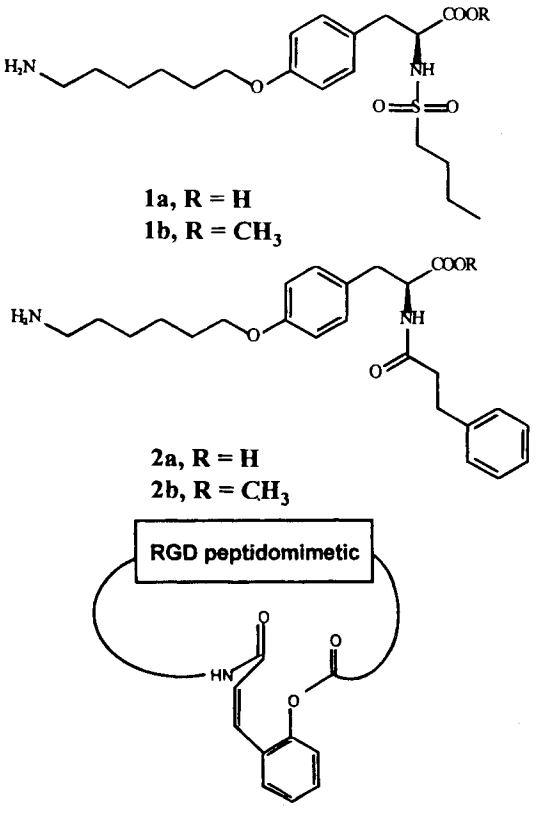

Fig. 1. RGD peptidomimetics and the corresponding prodrugs used in this study.

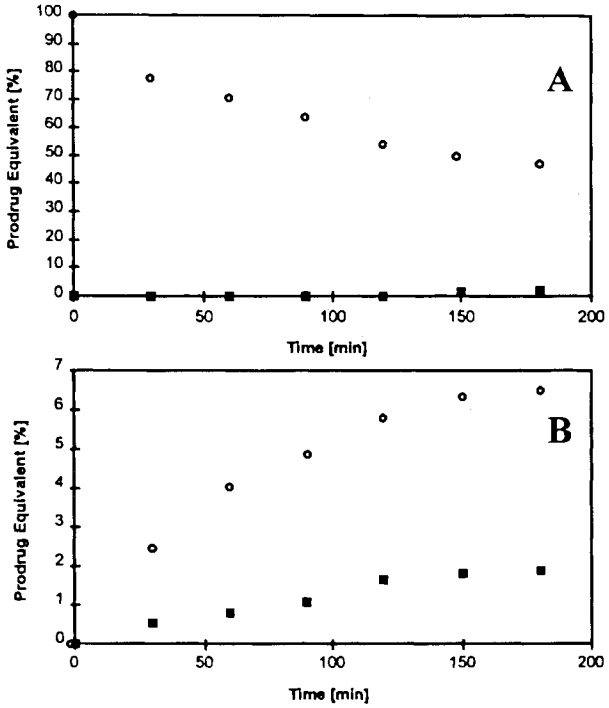

Fig. 2. Transport and metabolism of the coumarin-based cyclic prodrug 3a when applied to the AP side of Caco-2 cell monolayers and incubated for 3 h at 37°C. Panel A shows the time course of disappearance of prodrug 3a (○) and the appearance of the corresponding RGD peptidomimetic 1a (■) in the donor compartment; Panel B represents the amount of prodrug 3a (○) and RGD peptidomimetic 1a (■) appearing in the receiver compartment.

DISCUSSION

One of the primary goals of this study was to compare the membrane transport characteristics of linear and cyclic prodrugs of RGD peptidomimetics. A fundamental requirement for any successful prodrug strategy is reliable conversion to the parent drug by either enzyme-catalyzed or non-enzymatic reactions (23). Both prodrugs described here were designed to release the RGD peptidomimetic into the blood stream by esterase-mediated hydrolysis after successfully traversing the gastrointestinal epithelial barrier.

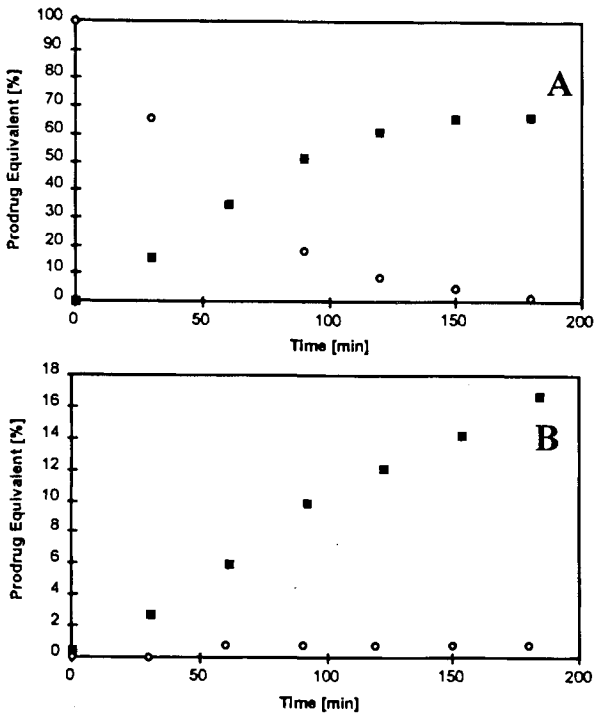

Fig. 3. Transport and metabolism of the methylester-based linear prodrug 1b when applied to the AP side of Caco-2 cell monolayers and incubated for 3 h at 37°C. Panel A shows the time course of disappearance of prodrug 1b (○) and the appearance of the corresponding RGD peptidomimetic 1a (■) in the donor compartment; Panel B represents the amount of prodrug 1b (○) and RGD peptidomimetic 1a (■) appearing in the receiver compartment.

To assess the susceptibility of the prodrugs to esterase-catalyzed hydrolysis, several biological media were selected. Based on the spectrophotometric assay using *p*-nitrophenol butyrate as a substrate, all biological media used in this study exhibited measurable levels of esterase activity (Tables I and II). The specific esterase activity in the biological media, however, was remarkably species-dependent, indicating that rat tissue exhibits much higher esterase activity than human tissues and media, respectively. Also, almost no esterase activity could be determined in aliquots of the HBSS buffer, pH 7.4, taken from the AP and BL sides of Caco-2 cell monolayers, indicating that, at least during the transport experiment (180 min), only small amounts of esterases were released from the cell monolayers.

Both cyclic RGD peptidomimetic prodrugs 3a and 3b, which used a coumarin promoiety, exhibited significantly higher permeation through Caco-2 cell monolayers compared to the parent RGD peptidomimetics 1a and 2a (Table III). In the receiver compartment, mainly unmetabolized prodrug was detected (Fig. 2B), indicating high enzymatic and chemical stability of these cyclic prodrug systems during the Caco-2 cell monolayer passage. Apparent half-lives of the cyclic prodrugs in 90% human blood plasma and rat tissue homogenate were significantly less than in HBSS, pH 7.4. This suggests that the disappearance of the cyclic prodrugs in these biological media may be catalyzed mainly by esterases. Additional experimental evidence for the proposed esterase-catalyzed reaction was obtained from studies using paraoxon, a potent esterase inhibitor [esterases that are sensitive to paraoxon are classified as B-esterases (24)]. Apparent half-lives of the cyclic prodrugs in 90% human plasma and rat tissue homogenate were significantly longer after preincubation with paraoxon. However, since the inhibition of the enzymatic hydrolysis was not complete in the presence of paraoxon, we conclude that these media contain not only B-esterases but also a certain amount of "non"-B-esterases (i.e., A- and/or C-esterases). However, carboxypeptidases are also known to hydrolyze ester bonds (25) and, therefore, it is not known whether the release of the parent peptidomimetics from the cyclic prodrugs is mediated only by esterases. These observations are in agreement with data published earlier by our laboratories (17). In Caco-2 cell homogenate, however, the rates of disappearance of the cyclic prodrugs in the absence of the potent esterase inhibitor were not significantly different from the chemical hydrolysis rate, in spite of the fact that this biological medium had high esterase activity (Tables I and II). This suggests that the cyclic prodrugs can be cleaved only by a certain family of isoenzymes that are present in 90% human plasma and rat tissue homogenate but not in Caco-2 cells.

For the linear methylester-based prodrugs 1b and 2b, the apparent permeation (when one considers the appearance of both the prodrug and the RGD peptidomimetic) through Caco-2 was even better than for the corresponding coumarin-based cyclic prodrugs (Table III). In contrast to the cyclic prodrugs, the linear methylester prodrugs generated the RGD peptidomimetics as the major component in the receiver compartment (Fig. 3B), indicating high metabolic and/or chemical instability of these prodrugs during the Caco-2 cell monolayer passage. The apparent half-lives in HBSS, pH 7.4, suggest a high chemical stability of the linear prodrug systems. Disappearance rates of the linear prodrugs in 90% human blood plasma, rat tissue homogenate, and Caco-2 cells were considerably faster than the rate of chemical hydrolysis. This suggests that the disappearance of the linear prodrugs in all these biological media may be catalyzed by esterases and/or carboxypeptidases. Based on the foregoing considerations it is quite likely that the methylester-based prodrugs can be hydrolyzed by different isoenzymes of esterases present in the different biological media. Again, additional experimental evidence for the proposed esterase-catalyzed reaction was obtained from studies using paraoxon. Apparent half-lives of the linear prodrugs in all these biological media were significantly longer after preincubation with paraoxon.

The intestinal mucosa represents a significant barrier to oral delivery of prodrugs into the systemic circulation (26). Tight intercellular junctions limit paracellular flux (physical barrier), lipoid membrane structures hinder transcellular permeation (physical barrier), and esterases associated with the brush-border membrane and/or the cytoplasm (metabolic barrier) metabolize esterase-sensitive prodrugs by releasing their parent drug. The existence of apically polarized efflux mechanisms may be an additional factor limiting membrane permeation (27). Active carrier-mediated membrane transport of compounds, on the other hand, may promote their absorption (28). In a number of studies it has been demonstrated that passive flux through a biomembrane is highly correlated to lipophilicity (also accounting for polarity and charge of the compounds) and molecular size (29,30). Therefore, it was of interest to investigate the transport characteristics of the prodrugs (and their parent RGD peptidomimetics) in Caco-2 cell monolayers, an *in vitro* model of the intestinal mucosa known to exhibit physical and metabolic barrier properties and active transport mechanisms similar to the situation *in vivo* (22,31–33), and to correlate

the results in the light of the physicochemical properties (Table IV) of the compounds considered (21).

The RGD peptidomimetics 1a and 2a used in this study disappeared very slowly from the AP side of the Caco-2 cell monolayers, indicating an unfavorable lipophilicity of these compounds, which limits their distribution into the lipophilic membrane. This observation is in agreement with data published earlier by other laboratories (3,5,6). In addition, the large molecular size of these compounds (Table IV) may prevent them from permeating via the paracellular tight junctional pathway (30). In contrast, the linear methylester-based prodrugs 1b and 2b as well as the cyclic coumarin-based prodrugs 3a and 3b exhibited a highly increased permeation through Caco-2 cells compared to the parent RGD peptidomimetics 1a and 2a when applied to the AP side of the monolayer. The molecular size, as revealed by NMR analysis, appears to be approximately the same for the RGD peptidomimetics and their corresponding methylester-based linear prodrugs (Table IV). The coumarin-based cyclic prodrugs however, seem to be only slighly larger. The molecular weight, a simple accessible molecular size descriptor (30), confirms these data derived from NMR experiments (Table IV). Therefore, the considerable increase in the membrane interaction potential [lipophilicity (34,35)] of the linear prodrugs (about 100-fold more lipophilic than the corresponding RGD peptidomimetics, Table IV) and of the cyclic prodrugs (about 240-fold more lipophilic than the corresponding RGD peptidomimetics, Table IV), respectively, seems to be the main factor influencing the change in their transport characteristics. However, while high lipophilicity may promote the distribution of a compound into the membrane, a potential disadvantage of highly lipophilic compounds may be their tendency to associate with the membrane and not to readily partition into the aqueous receiver compartment. Therefore, accumulation of compound within the cells may result.

To support the theory that the membrane interaction potential is the main factor influencing the membrane permeability of our compounds, the involvement of active transporters (efflux mechanisms and/or carriers) in the permeation process must be excluded. An efficient way to study the possible involvement of active transporters in the absorption process is to compare the permeability results from the transport experiments conducted through Caco-2 cells in both directions (AP-to-BL and BL-to-AP). If an active transport process is involved, the permeability coefficient should be dependent on the transport direction of the active transporter (27). Based on the results of the transport experiments in both directions conducted in this study (Table III), it can be assumed that neither the RGD peptidomimetics 1a and 2a nor the coumarin-based prodrugs 3a and 3b are substrates for active transporters. For the linear methylester-based prodrugs 1b and 2b, however, the involvement of an apically polarized efflux mechanism in their transport is very likely since the observed AP-to-BL transport is lower than that in the BL-to-AP direction.

In conclusion, both coumarin-based cyclic prodrugs were chemically less stable, but metabolically more stable, than the methylester-based linear prodrugs. The measured esterase stability of the cyclic prodrugs means that they are transported intact across the Caco-2 cell monolayer in contrast to the methylester prodrugs, which undergo facile bioconversion during their transport across the Caco-2 cell monolayer to the RGD peptidomimetics. However, based on the change in their physicochemical properties (mainly membrane interaction potential) both prodrug systems successfully delivered more (5-12-fold) of the RGD peptidomimetic and/or the precursor (prodrug) than did the RGD peptidomimetics themselves. But, how useful are these data in predicting the *in vivo* permeation of these prodrugs? While Caco-2 cells have been extensively used to measure the permeation of drugs and drug candidates, and these results correlate well with intestinal *in situ/in vivo* mucosa absorption (22,32,38), it is still unclear how useful this model is for studying prodrugs. Some examples have appeared in the literature (17,18,39); however, the correlation of these results with *in vivo* performance is lacking. Differences between *in vitro* and *in vivo* results may exist because of differences in levels of expression of esterases or the presence of esterases (lipases) in the intestinal lumen but not in Caco-2 cells. To properly interpret the meaning of the data generated in this study, similar experiments need to be done *in vivo*.

Table IV. Physicochemical Properties for the RGD Peptidomimetics 1a and 2a, the Methylester-based Prodrugs 1b and 2b, and the Coumarin-based Prodrugs 3a and 3b

Compound	Physicochemical Descriptors		
	r[Å][a]	MW[b]	log k_w(7.4)[c]
RGD Peptidomimetic 1a	4.75	401	1.22
Cyclic Prodrug 3a	4.96	529	3.60
Linear Prodrug 1b	4.75	415	3.21
RGD Peptidomimetic 2a	4.37	413	1.23
Cyclic Prodrug 3b	4.55	541	3.71
Linear Prodrug 2b	4.37	427	3.30

[a] Stokes-Einstein radius calculated from the diffusion coefficient determined by NMR in DMSO-d6 (17,21).
[b] Molecular weight as a simple accessible molecular size descriptor (30).
[c] Polycratic capacity factor determined from the partitioning of the solute between 0.01 M phosphate buffer (pH 7.4)/acetonitrile and an immobilized artificial membrane of phosphatidylcholine analogs (IAM.PC.DD) as a descriptor for the lipophilic membrane interaction potential of compounds (34,35). Values are extrapolated to 100% phosphate buffer (21,36,37).

ACKNOWLEDGMENTS

This research was supported by a grant from the Costar Corporation.

REFERENCES

1. G. D. Hartman, M. S, Egbertson, W. Halczenko, W. L. Laswell, M. E. Duggan, R. L. Smith, A. M. Naylor, P. D. Manno, R. J. Lynch, G. Zhang, C. T. Chang, and R. J. Gould. Non-peptide fibrinogen receptor antagonists. 1. Discovery and design of exosite inhibitors. *J. Med. Chem.* **35**:4640–4642 (1992).
2. D. R. Philips, I. F. Charo, L. V. Parise, and L. A. Fitzgerald. The platelet membrane glycoprotein IIb-IIIa complex. *Blood* **71**:831–843 (1988).
3. J. Zablocki, N. Nicholson, and B. Taite. Selection of an orally active glycoprotein IIb/IIIa receptor antagonist for clinical trials. *Thromb. Haemostas.* **69**:1244 (1993).
4. H. U. Stilz, B. Jablonka, M. Just, J. Knolle, E. F. Paulus, and G. Zoller. Discovery of an orally active non-peptide fibrinogen receptor antagonist. *J. Med. Chem.* **39**:2118–2122 (1996).
5. V. Austel, F. Himmelsbach, and T. Muller. Nonpeptidic fibrinogen receptor antagonists. *Drugs of the Future* **19**:757–764 (1984).

6. J. A. Zablocki, M. Miyano, R. B. Garland, D. Pireh, L. Schretzman, S. N. Rao, R. J. Lindmark, S. G. Panzer-Knodle, N. S. Nicholson, B. B. Taite, A. K. Salyers, L. W. King, J. G. Campion, and L. P. Geigen. Potent in vitro and in vivo inhibitors of platelet aggregation based on the Arg-Gly-Asp sequence of fibrinogen. A proposal on the nature of the binding interaction between the Arg-guanidine of RGDX mimetics and the platelet GP IIb-IIIa receptor. *J. Med. Chem.* **36**:1813–1819 (1993).
7. J. S. Barrett, G. Murphy, K. Peerlinck, I. DeLepeleire, R. J. Gould, D. Panbianco, E. Hand, H. Deckmyn, J. Vermylen, and J. Arnout. Pharmacokinetics and pharmacodynamics of MK-383, a selective non-peptide platelet glycoprotein-IIb/IIIa receptor antagonist, in healthy men. *Clin. Pharmacol. Ther.* **56**:377–388 (1994).
8. S. Vickers, C. A. Duncan, A. S. Yuan, and K. P. Vyas. Disposition of MK-852, a fibrinogen receptor antagonist, in rats and dogs. *Drug Metab. Dispos.* **22**:631–636 (1994).
9. T. Prueksaritanont, L. M. Gorham, J. D. Ellis, C. Fernandez-Metzler, P. Deluna, J. R. Gehret, K. L. Strong, J. H. Hochman, B. C. Askew, M. E. Duggan, J. D. Gilbert, J. H. Lin, and K. P. Vyas. Species and organ differences in first-pass metabolism of the ester prodrug L-751,164 in dogs and monkeys. In vivo and in vitro studies. *Drug Metab. Dispos.* **24**:1263–1271 (1996).
10. T. Prueksaritanont, L. M. Gorham, J. A. Naue, T. G. Hamill, B. C. Askew, and K. P. Vyas. Disposition of L-738,167, a potent and long-acting fibrinogen receptor antagonist, in dogs. *Drug Metab. Dispos.* **25**:355–361 (1997).
11. J. S. Barrett, R. J. Gould, J. D. Ellis, M. M. Holahan, M. T. Stranieri, J. J. Lynch, Jr., G. D. Hartman, N. Ihle, M. Duggan, O. A. Moreno, and A. D. Theoharides. Pharmacokinetics and pharmacodynamics of L-303,014, a potent fibrinogen receptor antagonist, after intravenous and oral administration in the dog. *Pharm. Res.* **11**:426–431 (1994).
12. N. B. Modi, S. A. Baughman, B. D. Paasch, A. Celnitur, and S. Y. Smith. Pharmacokinetics and pharmacodynamics of TP-9201, a GPIIb/IIIa antagonist, in rats and dogs. *J. Cardiovasc. Pharmacol.* **25**:888–897 (1995).
13. J. H. Hutchinson, J. J. Cook, K. M. Brashear, M. J. Breslin, J. D. Glass, R. J. Gould, W. Halczenko, M. A. Holahan, R. J. Lynch, G. R. Sitko, M. T. Stranieri, and G. D. Hartman. Non-peptide glycoprotein IIb/IIIa antagonists. 11. Design and in vivo evaluation of 3,4-dihydro-1(1H)-isoquinolinone-based antagonists and ethyl ester prodrugs. *J. Med. Chem.* **39**:4583–4591 (1996).
14. T. Weller, L. Alig, M. Beresini, B. Blackburn, S. Bunting, P. Hadvary, M. Hürzeler Müller, D. Knopp, B. Levet-Trafit, M. Terry Lipari, N. B. Modi, M. Müller, C. J. Refino, M. Schmitt, P. Schönholzer, S. Weiss, and B. Steiner. Orally active fibrinogen receptor antagonists. 2. Amidoximes as prodrugs of amidines. *J. Med. Chem.* **39**:3139–3147 (1996).
15. S. Gangwar, G. M. Pauletti, B. Wang, T. J. Siahaan, V. S. Stella, and R. T. Borchardt. Prodrug strategies to enhance the intestinal absorption of peptides. *Drug Disc. Today* **2**:22–29 (1997).
16. B. Wang, S. Gangwar, G. M. Pauletti, T. J. Siahaan, and R. T. Borchardt. Synthesis of a novel esterase-sensitive cyclic prodrug system for peptides that utilizes a trimethyl lock-facilitated lactonization reaction. *J. Org. Chem.* **62**:1363–1367 (1997).
17. G. M. Pauletti, S. Gangwar, F. W. Okumu, T. J. Siahaan, V. J. Stella, and R. T. Borchardt. Esterase-sensitive cyclic prodrugs of peptides: Evaluation of an acyloxyalkoxy promoiety in a model hexapeptide. *Pharm. Res.* **13**:1615–1623 (1996).
18. G. M. Pauletti, S. Gangwar, B. Wang, and R. T. Borchardt. Esterase-sensitive cyclic prodrugs of peptides: Evaluation of a phenylpropionic acid promoiety in a model hexapeptide. *Pharm. Res.* **14**:11–17 (1997).
19. B. Wang, W. Wang, and H. Zhang. Chemical feasibility studies of a potential coumarin-based prodrug system. *Bioorg. Med. Chem. Lett.* **6**:945–950 (1996).
20. B. Wang, W. Wang, H. Zhang, D. Shan, and T. D. Smith. Coumarin-based prodrugs. 2. Synthesis and bioreversibility studies of an esterase-sensitive cyclic prodrug of DADLE, an opioid peptide. *Bioorg. Med. Chem. Lett.* **6**:2823–2826 (1996).
21. B. Wang, W. Wang, G. Camenisch, J. Elmo, H. Zhang, and R. T. Borchardt. Coumarin-based prodrugs 4. Synthesis and evaluation of esterase-sensitive cyclic prodrugs of antithrombotic RGD analogs. *Bioorg. Med. Chem.*: submitted (1998).
22. I. J. Hidalgo, T. J. Raub, and R. T. Borchardt. Biochemical, histological and physicochemical characterization of human adenocarcinoma cells (Caco-2) as a model system for studying mucosal transport and metabolism of drugs. *Gastroenterology* **96**:736–749 (1989).
23. R. Oliyai. Prodrugs of peptides and peptidomimetics for improved formulation and delivery. *Adv. Drug Delivery Rev.* **19**:275–286 (1996).
24. W. N. Aldrige. Serum esterases. 1. Two types of esterase (A and B) hydrolysing *p*-nitrophenyl acetate, proprionate and butyrate, and a method for their determination. *Biochem. J.* **53**:110–117 (1953).
25. D. S. Auld and B. Holmquist. Carboxypeptidase A. Differences in the mechanism of ester and peptide hydrolysis. *Biochemistry* **13**:4355–4361 (1974).
26. G. M. Pauletti, S. Gangwar, G. T. Knipp, M. M. Nerukar, F. W. Okumu, K. Tamura, T. J. Siahaan, and R. T. Borchardt. Structural requirements for intestinal absorption of peptide drugs. *J. Controlled Rel.* **41**:3–17 (1996).
27. P. S. Burton, R. A. Conradi, A. R. Hilgers, and N. F. H. Ho. Evidence for a polarized efflux system for peptides in the apical membrane of Caco-2 cells. *Biochem. Biophys. Res. Commun.* **190**:760–765 (1993).
28. A. Tsuji, and I. Tamai. Carrier-mediated intestinal transport of drugs. *Pharm. Res.* **13**:963–977 (1996).
29. H. Van de Waterbeemd, G. Camenisch, G. Folkers, and O. A. Raevsky. Estimation of Caco-2 cell permeability using calculated molecular descriptors. *Quant. Struct. Act. Relat.* **15**:480–490 (1996).
30. G. Camenisch, H. Van de Waterbeemd, and G. Folkers. Review on theoretical passive drug absorption models. *Pharm. Acta Helv.* **71**:309–327 (1996).
31. P. Artursson. Cell cultures as models for drug absorption across the intestinal mucosa. *Crit. Rev. Ther. Drug Carrier Syst.* **8**:305–330 (1991).
32. S. Gan, C. Eads, T. Niederer, A. Bridgers, S. Yanni, P. H. Hsyu, F. J. Pritchard, and D. Thakker. Use of Caco-2 as an in-vitro intestinal absorption and metabolism model. *Drug Develop. Ind. Pharm.* **20**:615–631 (1994).
33. K. M. Hillgren, A. Kato, and R. T. Borchardt. In vitro systems for studying intestinal drug absorption. *Med. Res. Rev.* **15**:83–109 (1995).
34. S. Ong, H. Liu, X. Qiu, G. Bhat, and Ch. Pidgeon. Membrane partition coefficients chromatographically measured using immobilized artificial surfaces. *Anal. Chem.* **67**:755–762 (1995).
35. F. Barbato, M. La Rotonda, and F. Quaglia. Chromatographic indices determined on an immobilized artificial membrane (IAM) column as descriptors of lipophilic and polar interactions of 4-phenyldihydropyridine calcium-channel blockers with biomembranes. *Eur. J. Med. Chem.* **31**:311–318 (1996).
36. N. El Tayar, H. Van de Waterbeemd, and B. Testa. Lipophilicity measurements of protonated basic compounds by reversed-phased high-performance liquid chromatography. I. Relationship between capacity factors and the methanol concentration in methanol-water eluents. *J. Chromatogr.* **320**:293–304 (1985).
37. N. El Tayar, H. Van de Waterbeemd, and B. Testa. Lipophilicity measurements of protonated basic compounds by reversed-phased high-performance liquid chromatography. II. Procedure for the determination of a lipophilic index measured by reversed-phased high-performance liquid chromatography. *J. Chromatogr.* **320**:305–312 (1985).
38. A. R. Hilgers, R. A. Conradi, and P. S. Burton. Caco-2 cell monolayers as a model for drug transport across the intestinal mucosa. *Pharm. Res.* **7**:902–909 (1990).
39. P. Annaert, R. Kinget, L. Naesens, E. de Clerq, and P. Augustijns. Transport, uptake, and metabolism of the bis(pivaloxymethyl)-ester prodrug of 9-(2-phosphonyl-methoxyethyl)adenine in an in vitro cell culture system of the intestinal mucosa (Caco-2). *Pharm. Res.* **14**:492–496 (1995).